

Measurements of dipole and quadrupole polarizabilities of Rn-like Th⁴⁺

Julie A. Keele, Chris S. Smith, and S. R. Lundeen

Department of Physics, Colorado State University, Fort Collins, Colorado 80523, USA

C. W. Fehrenbach

J. R. Macdonald Laboratory, Kansas State University, Manhattan, Kansas 66506, USA

(Received 9 April 2012; published 21 June 2012)

Measurements of the fine structure pattern in high- L , $n = 37$ Rydberg levels of Th³⁺ have been extended and improved to allow more precise determinations of the dipole and quadrupole polarizabilities of the Rn-like Th⁴⁺ core of the Th³⁺ Rydberg system. The improved precision is partly due to the recent availability of theoretical calculations that limit the size of higher-order contributions to the fine structure pattern. The measured polarizabilities are $\alpha_D = 7.702(6)$ a.u. and $\alpha_Q = 29.1(1.9)$ a.u.

DOI: [10.1103/PhysRevA.85.064502](https://doi.org/10.1103/PhysRevA.85.064502)

PACS number(s): 32.30.Bv, 32.10.Dk, 32.10.Fn

The actinide elements typically occur in chemical compounds in high ionization states. Thorium, for example, usually occurs as Rn-like Th⁴⁺. Even though the properties of these ions are central to their chemical behavior, there are very few direct measurements of isolated ion properties that can serve as a check on the *a priori* predictions that are embedded in more complete chemical models. In the case of Th⁴⁺, measurements based on observations of high- L Rydberg fine structure patterns in Th³⁺ are beginning to provide such checks.

Measurements of the binding energy differences between $n = 37$ Rydberg levels of Th³⁺ with $9 \leq L \leq 15$ were recently reported [1], and used to infer the dipole and quadrupole polarizabilities of Th⁴⁺. We report here an extension and improvement of that study that leads to improved precision in the inferred polarizabilities. One improvement is the addition of the $L = 8$ to $L = 9$ interval to the data pattern. This leads to a much better limit on the curvature of the polarization plot, Fig. 3 in Ref. [1], and a corresponding improvement in the precision of the primary fit parameters. A second improvement in the data pattern was improved precision of the highest L intervals, the three-photon $L = 12$ to $L = 15$ interval and the two-photon $L = 12$ to $L = 14$ interval. These were improved by collecting more observations at a wider range of rf powers, improving the measured ac Stark shift of the 12–15 interval, which had limited the precision of the initial report. In addition to these improvements in the data pattern, theoretical calculations of the two parameters γ_D and δ , discussed in Ref. [1], were received [2] and incorporated in the analysis, reducing uncertainty from possible higher-order contributions to the fine structure pattern.

The measurement procedure was fully described in Ref. [1]. Briefly, a fast beam of Th³⁺ Rydberg ions is produced through charge capture by accelerated Th⁴⁺ ions from a selectively excited Rb Rydberg target. Individual L levels within the $n = 37$ manifold are selectively excited to a much higher n level by a CO₂ laser and the excitation is monitored by Stark ionization of the higher level. Resonant rf transitions between different L levels within $n = 37$, detected by their effect on the excitation, give precise information about the pattern of binding energies within the high- L $n = 37$ levels. Table I summarizes all the measured intervals.

Analysis of these measurements follows the procedure described in Ref. [1]. Table I shows the small correction for relativistic and second-order contributions to the measured intervals that were subtracted to infer the portion of each interval, $\Delta E^{[1]}$, that represents the expectation value of the long-range effective potential. These were scaled by the differences in hydrogenic expectation values of r^{-4} , and fit to the three-parameter function:

$$\frac{\Delta E^{[1]}}{\langle r^{-4} \rangle} = B_4 + B_6 \frac{\Delta \langle r^{-6} \rangle}{\Delta \langle r^{-4} \rangle} + B_8 \frac{\Delta \langle r^{-8} \rangle}{\Delta \langle r^{-4} \rangle}. \quad (1)$$

The results of this fit are illustrated in Fig. 1, showing a good fit across the entire range of intervals. The parameters returned by the fit were

$$B_4 = 3.8500(17), \quad B_6 = 6.59(50), \quad B_8 = 88(26).$$

The uncertainties in these parameters are from two to three times smaller than those reported in Ref. [1] from the smaller data set that lacked the 8–9 interval. The fitted curvature, represented by the parameter B_8 , is much smaller than was indicated by the smaller data set, and this has a corresponding effect on the initial slope parameter, B_6 .

The possible influence of stray electric fields within the rf interaction region was studied using the calculated Stark shift coefficients shown in Table I. Because the most significant Stark shifts occur in the highest L intervals, the presence of a stray electric field within the rf interaction region would cause a deviation of the highest L points (closest to the origin) from the straight line pattern in Fig. 1. Some previous studies have observed significant effects of such stray fields [3]. In contrast, the data in this study showed no indication of stray fields, and the quality of the fit was clearly reduced if a stray field as large as $\langle E^2 \rangle = 0.0010$ (V/cm)² was assumed [4]. The reduced stray field is likely due to the use of a different rf interaction region with a five-times-larger clear aperture, reducing the probability of charge deposition on surfaces within the rf region. In view of the stray field limit provided by the data pattern, an additional systematic uncertainty corresponding to an uncertainty of ± 0.0010 (V/cm)² in the mean squared stray electric field was applied to the fitted parameters. The additional uncertainties (± 0.0022 in B_4 and ± 0.45 in B_6) were comparable to the statistical uncertainties from the fit. In

TABLE I. Summary of measured intervals in $n = 37$ Rydberg levels of Th^{3+} . Column 1 shows the two L values whose binding energy difference is measured. Column 2 shows the net correction for ac shift applied in the case of multiphoton transitions. Column 3 shows the measured energy interval, in MHz. Columns 4 and 5 show the calculated contributions to the total interval from relativistic and second-order corrections. Column 6 shows the portion of the total interval due to the expectation value of the effective potential, $\Delta E^{[1]}$, which is fit to determine the polarizabilities. Column 7 shows the calculated Stark shift rate of each interval due to a possible stray electric field.

Interval	Δf_{AC} (MHz)	f_0 (MHz)	ΔE_{Rel} (MHz)	$\Delta E^{[2]}$ (MHz)	$\Delta E^{[1]}$ (MHz)	κ [MHz/(V/cm) ²]
8–9	0	1937.95(17)	10.96	7.18	1919.81(17)	– 13.6
9–10	0	1008.57(25)	8.88	1.96	997.73(25)	– 19.9
10–11	0	562.20(10)	7.33	0.61	554.26(10)	– 27.9
11–12	0	331.35(6)	6.16	0.21	324.98(6)	– 37.5
12–13	0	204.52(6)	5.25	0.08	199.19(6)	– 48.6
12–14	– 0.16(3)	335.70(7)	9.77	0.11	325.82(7)	– 109.3
12–15	– 0.74(16)	422.80(17)	13.71	0.12	408.97(17)	– 182.9

the report of Ref. [1] this uncertainty was omitted, resulting in a significant underestimate of the uncertainties in the inferred ion properties.

As discussed in Ref. [1], the parametrization of the data pattern through the fitted constants B_4 , B_6 , and B_8 , does not immediately yield estimates of the core polarizabilities because of the possible contributions from additional terms proportional to constants β_D , γ_D , and δ . The first two of these are very closely related to the dipole polarizability, and have been calculated with an estimated precision of $\pm 5\%$. The reported values for Th^{4+} are $\beta_D = 2.97(15)$ a.u. and $\gamma_D = 1.177(59)$ a.u., obtained with a theoretical method that successfully calculates α_D to within 1% [5]. The parameter δ is more problematic since it depends on products of dipole and quadrupole matrix elements among excited levels of Th^{4+} . Our early estimate of $\delta = 0 \pm 30$ a.u. [1] was based on theoretical line strengths [6] which did not specify the *signs* of the relevant matrix elements. In the meantime, full calculations of the relevant dipole and quadrupole matrix elements have been reported [5], and this allows for a much improved estimate. The excited states involved are the lowest seven odd excited

levels with $J = 1$ and the lowest eight excited levels with $J = 2$. The odd parity levels are in configurations $6p^{-1}6d$, $6p^{-1}7s$, and $6s^{-1}7p$, while the even parity levels are in configurations $6p^{-1}5f$, $6p^{-1}7p$, and $6s^{-1}6d$. Unfortunately, none of these levels has been observed experimentally, so both their energies and matrix elements had to be obtained from calculations. The method of calculation, the excitation energies, and some of the necessary matrix elements are reported in Ref. [5], but additional matrix elements were reported privately [2]. Using the reported energies and matrix elements, the parameter δ was calculated at two levels. The multiconfiguration Dirac-Fock (MCDHF) level gave the result $\delta = 16.8$ a.u., while the relativistic many body perturbation theory (RMBPT) level gave the result $\delta = 14.0$ a.u. Both are well within the bounds of our previous estimate. We will take the result to be $15.4(3.9)$ a.u., reflecting the difficulty of the calculation and absence of confirming measurements.

As previously reported [1], it is expected that the fit parameters B_4 and B_6 that describe the data pattern are related to the core polarizabilities α_D and α_Q by

$$B_4 = \frac{\alpha_D}{2} - [1.12(18) \times 10^{-3}] \gamma_D + [2.8(3) \times 10^{-5}] \delta,$$

$$B_6 = \frac{\alpha_Q}{2} - 3\beta_D + [1.18(6)] \gamma_D - [0.030(1)] \delta.$$

Here the coefficients of γ_D and δ are slightly different from those reported in Ref. [1] because they represent parametrization of the higher-order functions over a different range and with different relative weights. Substituting the fitted values of B_4 and B_6 , this leads to the conclusions

$$\alpha_D = 7.702(6) \text{ a.u.}, \quad \alpha_Q = 29.1(1.9) \text{ a.u.}$$

The precision of α_D (0.08%) is only slightly improved from Ref. [1] despite the factor of 2 improvement in the precision of the fit parameter B_4 . This is due to the more conservative treatment here of uncertainty due to possible stray electric fields. The precision of α_Q (6.5%) is a factor of 2 better than Ref. [1]. Both values reported here differ by approximately two standard deviations from the values reported in Ref. [1], probably due to the underestimate of the uncertainties in the previous report. The main difference from the previously reported values is a higher value of the

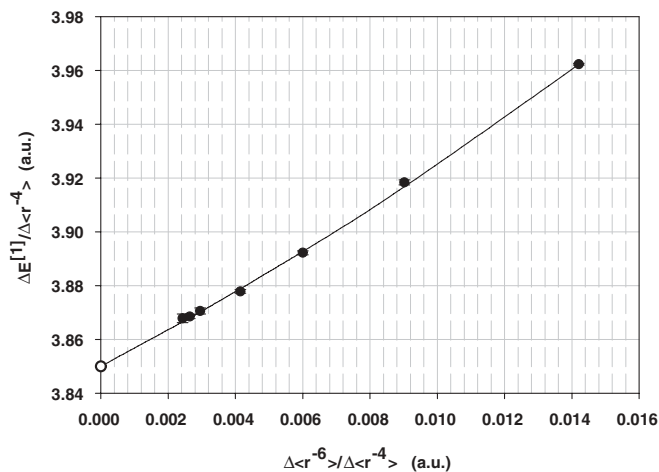


FIG. 1. Plot of the scaled first-order energy differences measured between high- L $n = 37$ Rydberg levels of Th^{3+} . The solid line shows the fit to Eq. (1) of the text. The fitted intercept, shown as an open circle, determines the dipole polarizability of the core ion Th^{4+} , while the initial slope determines its quadrupole polarizability.

TABLE II. Comparison of measured dipole and quadrupole polarizabilities of Rn-like Th^{4+} with representative calculations.

Property	Experiment	Theory
α_D (a.u.)	7.702(6) ^a	7.699 ^b
	7.720(7) ^c	7.75 ^d
	7.61(6) ^e	8.96 ^f
α_Q (a.u.)		10.26 ^g
	29.1(1.9) ^a	28.8 ^d
	21.5(3.9) ^c	24.5 ^f
	47(11) ^e	

^aThis work.

^bRCCSD(T); Reference [8].

^cReference [1].

^dRRPA; Reference [5].

^eReference [7].

^fDHF; Reference [5].

^gHartree-Fock; Reference [9].

quadrupole polarizability, due primarily to the extended data pattern that includes the $L = 8$ to $L = 9$ interval.

Table II compares these measurements with previous reports and with several representative calculations. Both measured polarizabilities agree to approximately 1% with calculations using the relativistic random-phase approximation (RRPA). This is well within the estimated 5% precision of those calculations. Even better agreement for the dipole polarizability is found with the calculation using the relativistic coupled-cluster [RCCSD(T)] method [0.04(8)%]. Calculations with the relativistic Dirac-Hartree-Fock (DHF) method are in error by more than 10% for both polarizabilities. Nonrelativistic calculations of α_D are in error by more than 30%.

The work reported here was carried out in the J. R. Macdonald Laboratory of Kansas State University. We are grateful for the cooperation of the laboratory staff and management. We thank both Donald Beck and Marianna Safronova for providing unpublished theoretical calculations. This work was supported by the Chemical Sciences, Geosciences, and Biosciences Division of the Office of Basic Energy Science, US Department of Energy.

[1] Julie A. Keele, S. R. Lundeen, and C. W. Fehrenbach, *Phys. Rev. A* **83**, 062509 (2011).

[2] M. S. Safronova (private communication).

[3] R. A. Komara, M. A. Gearba, S. R. Lundeen, and C. W. Fehrenbach, *Phys. Rev. A* **67**, 062502 (2003).

[4] Correcting the data for a field of 0.0010 (V/cm)^2 increased the reduced χ^2 of the fit from 1.5 to 2.1, reducing the probability by a factor of 3.

[5] U. I. Safronova and M. S. Safronova, *Phys. Rev. A* **84**, 052515 (2011).

[6] D. R. Beck (private communication).

[7] M. E. Hanni, J. A. Keele, S. R. Lundeen, and C. W. Fehrenbach, *Phys. Rev. A* **82**, 022512 (2010).

[8] P. Schwerdtfeger and A. Borschevsky (private communication).

[9] S. Fraga, J. Karwowski, and K. M. Saxena, *Handbook of Atomic Data* (Elsevier, Amsterdam, 1976).